

## Study of the beam-foil excitation mechanism with the use of chlorine projectiles, 2–10 MeV

C. Jupén, B. Denne, J. O. Ekberg, L. Engström, U. Litzén, I. Martinson, W. Tai-Meng, A. Trigueiros, and E. Veje\*

*Department of Physics, Lund University, Sölvegatan 14, S-223 62 Lund, Sweden*

(Received 1 June 1982)

Beam-foil excitation of chlorine projectiles has been studied by means of optical spectrometry, at projectile energies ranging from 2 to 10 MeV. The relative populations of various levels in Cl V through Cl VIII have been measured as functions of the projectile energy. It is concluded that for Cl VII and Cl VIII, the  $3p$  and  $3d$  terms are populated entirely through molecular-orbital (MO) electron promotions. High-lying levels of these charge states are excited by means of pickup of electrons from the valence band of the solid. Intermediate levels are populated through multiple inner-shell processes as well as from valence-band electron pickup. For Cl V and Cl VI, most of the levels are excited predominantly by pickup of electrons from the valence band. However, for some of the valence-shell levels in Cl VI, fairly strong contributions from MO processes are found at higher projectile energies. No evidence has been observed for direct Coulomb excitation.

### I. INTRODUCTION

This work is a continuation of our systematic studies of beam-foil excitation processes. For multiply ionized projectiles, we have recently observed<sup>1–3</sup> a fairly selective excitation of levels with  $n^* \simeq Z_{\text{core}}$ ,  $n^*$  being the effective quantum number of the excited level, and  $Z_{\text{core}}$  is the charge state of the core. In addition, for Ar VIII (Ref. 2) and Xe VIII (Ref. 3) strong excitations were observed for the valence-shell levels. The results of Refs. 1–3 indicate the presence of two excitation mechanisms. The high-lying levels are populated by pickup of electrons from the valence band of the foil when the projectile leaves the back of the foil, and the low-lying, valence-shell, levels are populated through inner-shell, molecular-orbital (MO), electron-promotion processes.

At the same time as the presence of such two distinctly different processes became established, new problems could be formulated.<sup>1–3</sup> For example, the two different excitation mechanisms may be active in populating one level at the same time. For such cases, it will be worthwhile to study how the relative degrees of the two processes will change with the projectile energy as well as with the charge state of the projectile. Another problem comes up for levels whose binding energies are so large that pickup of electrons from the valence band of the foil is relatively improbable, due to the large change in binding energy, at the same time as the levels have

so high excitation energies that they are not expected to become excited directly from MO processes. Will such levels become excited only from pickup of valence-band electrons, or will they also attain excitation from two-step, or multiple-step, inner-shell processes? Also, will Coulomb excitation occur?

To study such points, we have performed measurements with chlorine projectiles in the projectile energy range 2–10 MeV and measured changes in relative level populations versus the projectile energy for a number of levels in Cl V–Cl VIII. Some of the results, namely, excitation of the  $3p$  and  $3d$  levels in Cl VII and Cl VIII have already been published in a preliminary report.<sup>4</sup>

The studies referred to above<sup>1–3</sup> concentrated on the relative population of excited terms in alkali-like species as functions of the principal quantum number  $n$  and the orbital angular momentum quantum number  $l$  of the excited term at a fixed projectile energy.

### II. EXPERIMENTAL PROCEDURE, DATA TREATMENT, AND RESULTS

The measurements were done at the 3-MV Pelletron tandem accelerator at the Department of Physics, Lund University. The experimental procedure as well as the data treatment used here have been described before,<sup>1–4</sup> and the experimental

equipment is described in Ref. 5. Therefore, only a brief description will be given here.

Chlorine projectiles were accelerated to energies between 2 and 10 MeV and sent through thin (approximately  $5 \mu\text{g}/\text{cm}^2$ ) carbon foils. Photons emitted from the projectiles were analyzed by a 1-m normal incidence vacuum monochromator working in the wavelength region 40–600 nm. The computer-controlled<sup>5</sup> step motor of the monochromator was advanced from a beam integrator, so that signals obtained at different wavelengths were normalized to the same amount of beam charge measured with a foil in the beam path.

The spectral region from 58 to 83 nm was scanned with a resolution of 0.1 nm or better at projectile energies of 2, 4, 5.5, 7, and 10 MeV. At each projectile energy the beam current was measured in a Faraday cup located downstream from the foil with, as well as without a foil in the beam path, so that signals measured at different projectile energies could be normalized to the same number of projectiles.

The beam-foil spectrum of chlorine has recently been studied in our laboratory for spectroscopic purposes.<sup>6</sup> We have here extracted additional information from the previously<sup>6</sup> recorded spectrograms by normalizing them to the above-mentioned ones. In that way, information from other wavelength regions has been obtained. Also, a few scans previously<sup>6</sup> carried out at 4.9 and 6.6 MeV have been used here.

The relative population  $N_j$  of level  $j$  is basically given by<sup>7</sup>

$$N_j = S(\lambda_{jk}) / [K(\lambda_{jk})A_{jk}v], \quad (1)$$

where  $S(\lambda_{jk})$  is the signal at wavelength  $\lambda_{jk}$  of the optical transition from level  $j$  to level  $k$ ,  $K(\lambda_{jk})$  is the overall quantum efficiency of the detecting device,  $A_{jk}$  is the transition probability, and  $v$  is the projectile velocity. However, since in this work we were primarily interested in relative changes of level populations versus the projectile energy, Eq. (1) was reduced to

$$N_j = S(\lambda_{jk}) / v. \quad (2)$$

The validity of the application of Eqs. (1) and (2) has been discussed in Refs. 1, 2, and 7.

For most of the transitions studied in Cl V, Cl VI, and Cl VIII, the transition probabilities are not known sufficiently well. Therefore, Eq. (1) could not be applied to the data; only the change of level population as a function of the projectile energy was determined, cf. Eq. (2). For Cl VII (sodiumlike

chlorine) transition probabilities calculated in the numerical Coulomb approximation are available.<sup>8</sup> The relative population of various levels in Cl VII was determined as a function of the level binding energy, by use of Eq. (1). The result was in agreement with what has been observed previously for other multiply ionized species,<sup>1–3</sup> namely, that for Cl VII, the  $3p$  and  $3d$  levels are strongly excited, and also that levels with binding energies of approximately 8–10 eV (corresponding to  $n \simeq 8–10$ ) are strongly populated, whereas there is a minimum in population for levels with  $n \simeq 4–5$ . Since the relative level population feature for Cl VII qualitatively is much like that previously published<sup>2</sup> for Ar VIII, it is not presented here. For Cl VIII a similar feature was observed, especially a strong excitation of some high-lying levels, but a detailed, quantitative evaluation of the relative level population as a function of the level excitation energy was impossible, owing to lack of reliable transition probabilities.

The relative population of various levels in Cl V through Cl VIII, evaluated by means of Eq. (2), are in Figs. 1–6 plotted versus the projectile energy. Data for different levels are on different scales. In some of the figures are included data obtained at energies below 2 MeV, taken from Ref. 9. Such data are represented by smooth curves without data points, and the curves have been normalized to ours at 2 MeV.

The relative uncertainty related to each point is normally between 10% and 20%. As we shall see, the sometimes fairly large relative uncertainties shall not prevent us from a detailed discussion of the results.

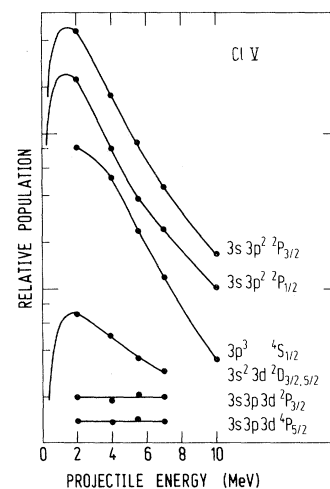


FIG. 1. Relative level populations for some levels in Cl V plotted semilogarithmically vs the projectile energy.

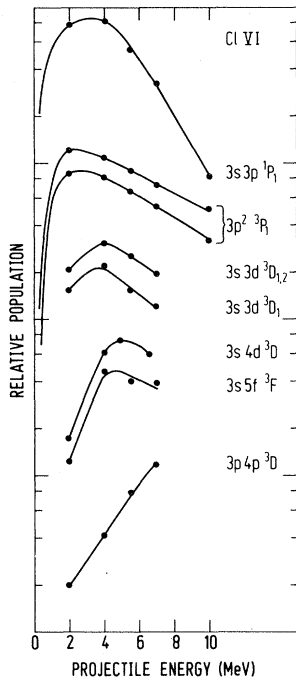


FIG. 2. Relative level populations for some levels in Cl VI plotted semilogarithmically vs the projectile energy.

In some cases we could observe two transitions from the same upper level. The two population curves (i.e., curves showing relative change of level population versus the projectile energy) agreed normally, confirming our uncertainty estimates. As an example, see the two population curves for the  $3p^2 3P_1$  level in Cl VI, Fig. 2. Also, population

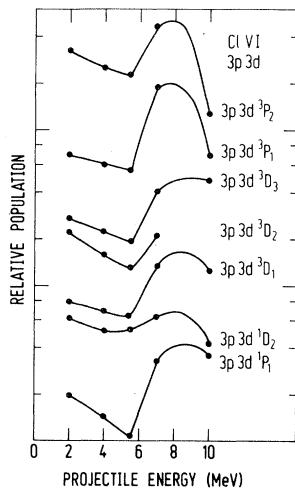


FIG. 3. Relative level populations for some levels of configuration  $3p3d$  in Cl VI plotted semilogarithmically vs the projectile energy.

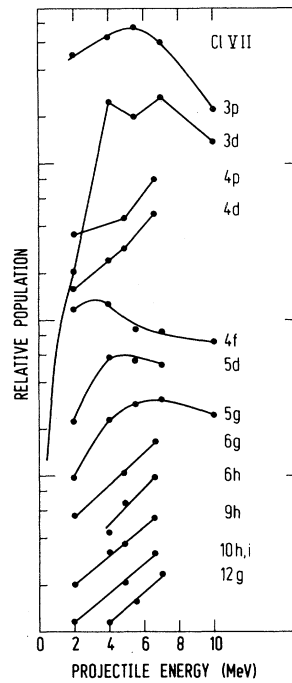


FIG. 4. Relative level populations for some levels in Cl VII plotted semilogarithmically vs the projectile energy.

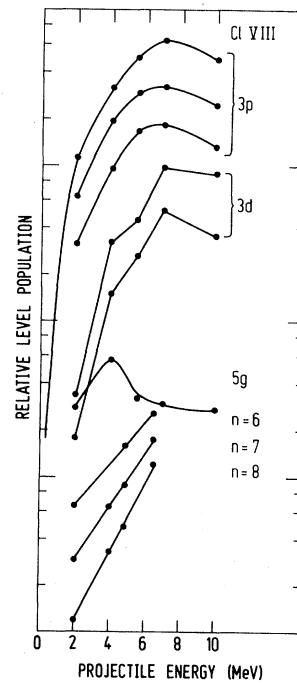


FIG. 5. Relative level populations for some levels in Cl VIII plotted semilogarithmically vs the projectile energy.

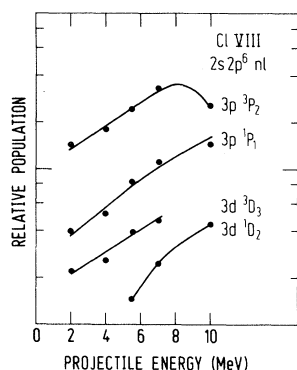


FIG. 6. Relative level populations for some levels of configuration  $2s 2p^6 3p$  or  $2s 2p^6 3d$  in Cl VIII plotted semi-logarithmically vs the projectile energy.

curves for different levels of the same upper term were generally found to be proportional, as expected. For an example, see the data for the  $3s 3p^2 2P_{1/2}$  and the  $3s 3p^2 2P_{3/2}$  levels in Cl V, Fig. 1. However, as is obvious from Figs. 1–6, levels of the same charge state, but belonging to different configurations may well show quite different population curves, and the change of slope or shape of the population curves may well exhibit irregular features (see Figs. 3–6). These are important findings and a lengthy discussion shall be given in Sec. III.

### III. DISCUSSION

It has been mentioned repeatedly in the literature (see, e.g., Refs. 1–3 and 10) that excited projectile levels, whose mean diameter is comparable to or larger than the average distance between nearest neighbor foil atoms, cannot exist as long as the projectile is inside the foil. The excitation of such levels must take place when the projectile leaves the foil. On the other hand, levels of small size compared to the distance between foil atoms may survive over fairly large distances during the passage through the foil. These facts are of importance for the following discussion.

For Cl VII and Cl VIII (sodiumlike and neonlike chlorine) we observe that the curves for the  $3d$  levels increase at low projectile energies much more steeply with increasing projectile energy than the  $3p$  curves (Figs. 4 and 5). This has already been discussed in a preliminary publication,<sup>4</sup> the conclusion being that the  $3p$  and  $3d$  levels in Cl VII and Cl VIII are excited through transfer of a carbon  $1s$  electron to the state in question. The transfer process was described<sup>4</sup> in terms of the molecular-orbital (MO) electron-promotion picture.<sup>11,12</sup> The starting point

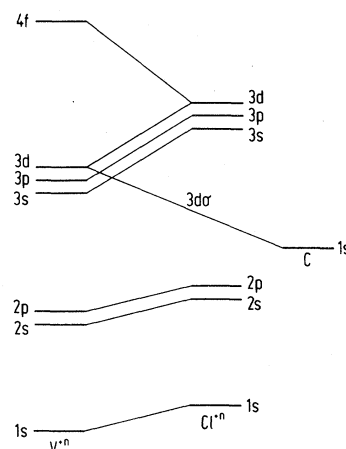


FIG. 7. Diabatic molecular-orbital diagram for the chlorine-carbon collision shown schematically. To the right of the figure is shown the inner-shell terms of the separated atoms (not to scale), and the united-atoms inner-shell terms are given to the left (not to scale). The terms of the separated and the united atoms have been connected by straight lines to indicate how the levels correlate during a collision. For a detailed discussion of the correlation diagram, see Ref. 4.

for such a discussion is the so-called MO correlation diagram,<sup>11</sup> which is a schematic representation of how the various subshells of the free collision partners correlate to the different subshells of the united atoms. The correlation diagram for the carbon-chlorine collision is shown in Fig. 7. The construction and the validity of the diagram are discussed in Ref. 4. The detailed discussion<sup>4</sup> of the  $3p$  and  $3d$  level excitations in Cl VII and Cl VIII shall not be repeated here, but only the aforementioned conclusion, namely, that a  $1s$  carbon electron can be transferred to the  $3p$  term in the projectile through a MO radial coupling taking place at a finite internuclear distance (cf. Fig. 7), whereas the  $3d$  term is populated through a rotational coupling in the united atoms limit (Fig. 7). The rotational coupling is less efficient than the radial coupling at low projectile energies, partly because the relatively short internuclear distance necessary for the rotational coupling to be active is only reached in rather few collisions with small impact parameters, and partly because the angular velocity entering the rotational coupling transition probability<sup>12</sup> is reduced at low projectile velocities. Both factors reduce the  $1s$ - $3d$  MO process at low projectile energies, making the  $3d$  population curves steeper than the corresponding  $3p$  curves.

It must be mentioned here that the MO mechanism will also populate the  $3s$  levels in Cl VII and Cl VIII, in addition to the  $3p$  and  $3d$  levels. Howev-

er, the  $3s$  level in Cl VII is the ground state so its population cannot be measured by optical detection, and also—unfortunately enough—we were unable to observe the  $2p$ - $3s$  transitions in Cl VIII. But, according to the correlation diagram (Fig. 7), a  $1s$  carbon electron can be transferred to the  $3s$  projectile level as well as to the  $3p$  or  $3d$  configurations. Also, the  $1s$ - $3s$  transfer probability will most presumably be relatively strong, since a radial coupling, located at a fairly large internuclear separation, is involved.

In Fig. 8 is plotted the ratios between the  $3p$  and  $3d$  level populations for Cl VI-VIII in arbitrary units. The similarity between the Cl VII and Cl VIII data is noteworthy, leading to the conclusion that the same mechanism (i.e., the MO electron promotion mechanism) is active for Cl VII and Cl VIII. However, the  $3p$  to  $3d$  population ratio for Cl VI, also given in Fig. 8, differs clearly from those for Cl VII and Cl VIII. This indicates a change in excitation mechanism with charge state. Although the MO mechanism may be responsible in part for the  $3s$ ,  $3p$ , and  $3d$  level populations in Cl VI, another mechanism is not only present, but seems to be dominating for these levels in Cl VI. This mechanism is undoubtedly pickup of electrons from the foil valence band. This is supported by another finding, namely, that the triplets in Cl VI are excited with similar or greater strengths than the corresponding singlets. Were the MO electron-promotion mechanism responsible for the  $3s$ ,  $3p$ , and  $3d$  excitations in Cl VI, then one would expect only singlets in Cl VI to become populated noticeably. This is owing to the Wigner spin conservation rule.<sup>13</sup> If, during the course of an atomic collision, the spin-orbit interaction is weak, the total electronic spin is conserved.

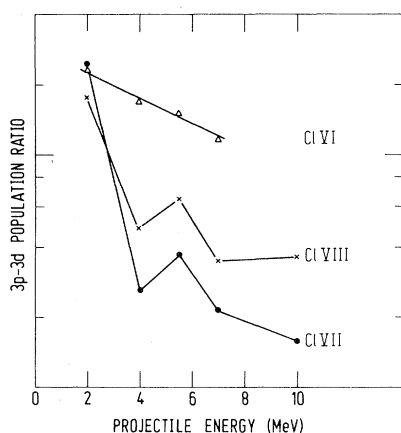


FIG. 8. Ratios of  $3p$  to  $3d$  level populations (in arbitrary units) in Cl VI, Cl VII, and Cl VIII plotted semilogarithmically vs the projectile energy.

Therefore, transfer of both of the  $1s$  carbon electrons can only lead to excitation of singlet levels, because the  $1s^2$  electrons in carbon initially form a singlet structure. Population of a triplet level in Cl VI would imply the presence of a strong spin-orbit interaction during the collision, which is unlikely. The presence of pickup of electrons from the foil valence band to the  $3s$ ,  $3p$ , and  $3d$  configurations in Cl VI is in accordance with a previous study<sup>14</sup> of S VI, in which it was found that the  $3p$ ,  $3d$ , and  $5f$  levels have proportional population curves.<sup>4,14</sup> Clearly the levels in S VI were populated by the same mechanism, which, owing to the fairly large size of approximately 5 a.u. for the mean radius of the  $5f$  orbital (scaled hydrogenic mean radius), must be electron pickup from the valence band of the foil, taking place at the exit of the foil.

The creation of a  $2p$  vacancy in Cl VIII seems to be caused by a mechanism not related to the MO processes feeding the  $n=3$  configurations in Cl VIII. This is concluded not only from the similarities between the  $3p$  to  $3d$  population ratios for Cl VII and Cl VIII as shown in Fig. 8, but also from the Wigner spin conservation rule.<sup>13</sup> The levels of configurations  $2p^5 3p$  and  $2p^5 3d$  in Cl VIII are generally not described well in the  $LS$ -coupling limit. Rather, a pair coupling is relevant.<sup>6</sup> This implies that, for most of the levels of these two configurations, the total electronic spin cannot be specified. However, that level of each configuration with the highest value of the total angular momentum has a pure triplet nature. This is simply because the highest possible value of the total angular momentum can only be reached if both the orbital angular momenta and the spins of the two unpaired electrons are coupled parallel. But since the complete  $2p^6$  core is a singlet, the above-mentioned two triplets cannot result from direct excitation of a  $2p$  electron, due to the Wigner spin conservation rule. The two levels of pure triplet nature are excited strongly, and their population functions are proportional to the population functions of the other levels of the same configuration. These findings indicate that direct excitation of a  $2p$  electron is nonimportant. Rather, we conclude that the  $2p$  electron is transferred to a continuum state (Coulomb ionization) and a  $1s$ - $3p,d$  MO process is acting in addition. Whether these two independent steps take place in the same collision or they result from two adjacent collisions cannot be said at present.

The conclusion that direct excitation is nonimportant is specific for the collision studied here, and is not of general nature. Direct MO electron-

promotion from one shell to another in the same atom can well occur in other collisions, but whether Coulomb excitation to a final bound state can take place with an appreciable probability is not so well established yet.

For excitation of the Cl VIII levels of configuration  $2s2p^63p$  or  $3d$ , similar considerations can be applied for the triplet levels (cf. Fig. 6) with the result that the population of these levels does not occur as a direct  $2s$ - $3p,d$  excitation. The  $2s$  vacancy is created by Coulomb ionization, and a MO process is responsible for the  $n = 3$  level population.

For the Cl VI levels of configuration  $3p3d$  we observe for each of the population curves a maximum at a projectile energy close to 8 MeV. However, there must be another maximum on each population curve, located at an energy below 2 MeV (see Fig. 3). Such a double-maximum feature is surprising and has not been observed before. Since the triplet levels are populated with similar strengths as the singlet levels, and because the population functions for the different levels of the  $3p3d$  configuration are rather close to being proportional, it can be said that both excitation of the  $3p$  and the  $3d$  electrons cannot result from a one-collision MO electron-promotion process. Again, this is a conclusion based on the Wigner spin conservation rule.<sup>13</sup> Neither can the capture of two electrons from the foil valence band account for both of the maxima in the population curves given in Fig. 3. Two electrons transferred from the valence band to the projectile will be caught essentially independent of each other.<sup>10</sup> This is partly because of the fairly high charge of the projectile core, implying that the mutual electron-electron repulsions will be relatively small, and partly because of the abrupt change in potential experienced by the electrons when leaving the foil.<sup>10</sup> Therefore, capture of two valence-band electrons will cause not more than one maximum in a population curve. The occurrence of two maxima on the population curves given in Fig. 3 can be explained as resulting from a combination of the two different excitation mechanisms: (i) capture of valence-band electrons and (ii) MO electron promotions.

At low projectile energies, any MO process probability will be relatively small, cf. the  $3p$  and  $3d$  excitations in Cl VII and Cl VIII, Figs. 4 and 5. Thus, the first maximum (i.e., that located below 2 MeV) shall find its explanation in terms of capture of two electrons from the foil valence band. However, at increasing projectile energy there will be an increasing probability for some of the projectiles initially stripped to charge state  $7+$  (neonlike) to

have experienced a violent collision inside the foil, resulting in a  $3p$  (preferentially) or  $3d$  (less probably) MO electron-transfer process, so that the projectile occurs as Cl VII excited to the  $3p$  or  $3d$  level when it enters the foil exit region. Then, when leaving the back of the foil, it may capture another electron. Such a combination of the two different population mechanisms can account for the maximum located at around 8 MeV. For the  $3s3p^2$  configuration in Cl V, a small kink is seen in the fairly steeply decreasing sections of the population curves at high energies, see Fig. 1. This may also reflect a contribution from a MO process at high projectile energies. The population curves for the  $3s3p3d$  levels in Cl V are remarkably independent of the projectile energy from 2 to 7 MeV (Fig. 1). Clearly, for this configuration, the two different population mechanisms counteract each other.

For the excitation of levels with  $n$  larger than 3 in Cl VII, we observe that the  $4p$  and  $4d$  population curves are fairly steeply increasing functions of the projectile energy (Fig. 4). Then, there is a drastic change of curve shape when turning to the population curve for the  $4f$  level, which has a maximum slightly below 4 MeV, and flattens out rather much at higher energies. For the  $5d$  and  $5g$  curves, the location of the maximum has shifted to higher projectile energies, and for the higher-lying levels ( $n = 6-12$ ), a steady increase in population versus the projectile energy is observed. The  $4p$ ,  $4d$ , and  $4f$  levels have binding energies of 51, 44, and 42 eV, respectively,<sup>8</sup> whereas the binding energies for the  $5d$  and  $5g$  terms are 28 and 27 eV, respectively.<sup>8</sup> Thus, the drastic change in population curve shape, occurring by going from the  $4d$  to the  $4f$  level, cannot be explained in terms of change of the level binding energy.

The  $4f$  and higher-lying levels in Cl VII are undoubtedly populated by capture of a foil valence-band electron at the back of the foil. For electron capture from a gaseous target atom to a projectile, it has been observed<sup>15</sup> that the maximum in total capture cross section as a function of the projectile energy shifts towards higher projectile energy, when the binding energy of the final level is decreased. The gradual shifts in shape and location of the maximum in the population curves for the  $4f$  and higher-lying levels in Cl VII is clearly the same feature as that observed in gas collisions.<sup>15</sup> The higher the excitation energy of the final level is, the higher in projectile energy will the maximum in electron capture probability be located.

For Cl VI (Fig. 2) and for the  $5g$  and higher-lying levels in Cl VIII (Fig. 5) very similar systematics are

observed as those found for the  $4f$  and higher-lying levels in Cl VII, supporting our explanation. Note also, that the  $4f$  level in Cl VII and the  $5g$  level in Cl VIII have rather similar population curves. This is understandable, because these two levels, in adjacent charge states, have very similar binding energies.<sup>6,8</sup>

The systematic change of the shape of the population curves seen in Cl VII for the  $4f$  and higher-lying levels (Fig. 4), in Cl VI (Fig. 2) and in Cl VIII for the  $5g$  and higher-lying levels (Fig. 5), leaves the  $4p$  and  $4d$  population curves in Cl VII as a peculiar case. If these two levels were populated predominantly through electron capture from the foil valence band, then one would expect a maximum in the population curves at a fairly low projectile energy. However, they are steadily increasing versus the projectile energy, so this is ruled out in our projectile energy range. On the other hand, the population curves must have a shoulder at a projectile energy below or around 2 MeV, cf. Fig. 4. That indicates the presence of valence-band electron capture at low energies, in accordance with the systematics observed for the higher-lying levels in Cl VII, but leaves the steady increase in population unexplained. Also, as seen from the MO correlation diagram in Fig. 7, no one-step inner-shell electron-promotion process can be expected to be active in populating these two terms, because there are no curve crossings with electron-carrying curves leading to the  $4p$  or  $4d$  terms. In addition, long-range couplings between the molecular potential energy curves dissociating to the  $n = 3$  and the  $n = 4$  terms are unlikely to produce electron promotion to an  $n = 4$  level late in the collision, because the molecular potential energy curves are well separated in energy (the  $4p, d$  levels in Cl VII are approximately 30 eV above the  $3d$  level).

The peculiarity of the population curves for the  $4p$  and  $4d$  terms in Cl VII can plausibly be explained in terms of multiple collisions. An electron can be transferred to an  $n = 3$  state through a MO electron promotion taking place somewhere inside the foil during a violent collision. Then, in a later collision, the electron can be promoted further, from the  $n = 3$  to an  $n = 4$  level. The first collision will, on the average, favor the population of the  $3s$  level, leaving the  $3d$  level least populated. In the second collision, the  $3s$  level will be disturbed most easily and the  $3d$  level will receive the least disturbance, because of the sizes of the mean radii of these orbitals. Thus, excitation in the second collision will, in most cases, start from the  $3s$  state, with smaller probability from the  $3p$  level, and with least proba-

bility from the  $3d$  term. If, during the second collision, the number of nodes in the radial part of the wave function (equal to  $n - l - 1$ ) is conserved—and this is a corner stone in the theory for molecular correlation diagrams<sup>11,12,16</sup>—then the  $4f$  level will not become nearly as excited through multiple collisions as the  $4p$  and  $4d$  levels will. This is in agreement with the abrupt change in population curve shape between the  $4d$  and the  $4f$  levels (Fig. 4). From a detailed inspection of the  $4f$  and  $5g$  population curves in Cl VII it can be seen that the  $4f$  curve flattens out at high projectile energies. A similar hesitation to decrease is not found in the  $5g$  curve and may be caused by a contribution from multiple excitations for the  $4f$  term, which will be relatively more active at high projectile energies.

The structure seen in the population curves for the  $3d$  configurations in Cl VII and Cl VIII (Figs. 4 and 5) cannot be explained as resulting from valence-band electron pickup and MO electron promotions, respectively. The  $3d$  levels in Cl VII and Cl VIII have such large binding energies that electron pickup from the valence band to these levels is very improbable. Also, the  $3p$  to  $3d$  population ratios are very similar for Cl VII and Cl VIII, as demonstrated in Fig. 8. Were the levels fed from pickup of a valence-band electron, larger differences would have been expected, because valence-band electron pickup will peak at a lower projectile energy for Cl VII than for Cl VIII.

A possible explanation of the structures seen in the  $3d$  population curves for Cl VII and Cl VIII is that the foils contained some impurity, e.g., nitrogen or oxygen. The MO correlation diagrams for chlorine-nitrogen or chlorine-oxygen collisions will be similar to that for the chlorine-carbon collision (Fig. 7). Promotion of the  $1s$  electrons from nitrogen or oxygen will peak at higher projectile energies than for carbon due to the increased binding energy of the  $1s$  electrons. Thus, one might interpret the maxima seen at the higher projectile energy as being caused by presence of such impurities. However, one would expect the impurity to create a similar, second maximum in the  $3p$  population curves in Cl VII and Cl VIII, and that is not observed, cf. Figs. 4 and 5. Thus, an explanation in terms of presence of some impurity seems to be ruled out.

Possibly, but unlikely, the  $3d$  population curve structure can be explained in terms of the Rosenthal model,<sup>17,18</sup> which has been very successful in explaining oscillatory structure in total Rydberg-state excitation cross sections in several ion-atom collision systems (see, e.g., Ref. 19 and references given therein). The Rosenthal model<sup>17,18</sup> assumes that

two exit channels of the temporary molecular complex are coherently excited from the initial channel, usually, but not necessarily, by curve crossings. Also, a rotational coupling in the united atoms limit may be involved. Then, at a late stage in the collision, or, in other words, at a fairly large internuclear separation, the two coherently excited terms mix either through term approach or through a crossing with a third term. This can cause oscillations in the total cross sections versus the projectile energy, for the terms involved. Such a phenomenon is well established to occur for outer-shell excitations in ion-atom collisions (see, e.g., Ref. 19). In addition, basically the same feature has been observed in ion yields of  $\text{He}^+$  scattered on solid surfaces.<sup>20-22</sup> However, such an explanation seems to be unlikely for our results, because, although the  $3s$ ,  $3p$ , and  $3d$  terms can become coherently excited according to the MO correlation diagram (Fig. 7), there will be no interaction among these terms at a large internuclear separation, neither will the terms cross another common term late in the collision. Furthermore, the most likely candidate to interfere with the  $3d$  potential energy curve will be the  $3p$

curve, but no structure is observed in the  $3p$  excitations (cf. Figs. 4 and 5). Therefore, an explanation in terms of the Rosenthal model is not plausible.

A much more reasonable explanation of the  $3d$  population curve structures is in terms of multiple collisions. One of the maxima reflects the one-step  $1s$ - $3d$  MO electron promotion, and the other one reflects a contribution from a two-step collision process, in the first of which an electron is promoted from the carbon  $K$  shell to the  $3s$  or  $3p$  level in the projectile. Then, in the second collision, the electron is promoted further to the  $3d$  level.

#### ACKNOWLEDGMENTS

One of us (E.V.) is grateful to the Department of Physics, Lund University, for the hospitality he enjoyed during his stay, as well as for financial support from the Nordic Committee for Accelerator-Based Research. The work was also supported by the Swedish Natural Science Research Council (NFR) and the National Swedish Board for Energy Source Development (NE).

\*Present address: Physics Laboratory II, H.C. Ørsted Institute, Universitetsparken 5, DK-2100 Copenhagen, Denmark.

<sup>1</sup>B. Andresen, B. Denne, J. O. Ekberg, L. Engström, S. Huldt, I. Martinson, and E. Veje, *Phys. Rev. A* **23**, 479 (1981).

<sup>2</sup>S. Bashkin, H. Oona, and E. Veje, *Phys. Rev. A* **25**, 417 (1982).

<sup>3</sup>R. Hallin, J. Leavitt, A. Lindgård, P. Rathmann, H. Vach, and E. Veje (unpublished).

<sup>4</sup>C. Jupén, B. Denne, J. O. Ekberg, L. Engström, U. Litzén, I. Martinson, W. Tai-Meng, A. Trigueiros, and E. Veje (unpublished).

<sup>5</sup>L. Engström, B. Denne, S. Huldt, J. O. Ekberg, L. J. Curtis, E. Veje, and I. Martinson, *Phys. Scr.* **20**, 88 (1979).

<sup>6</sup>C. Jupén (unpublished).

<sup>7</sup>N. Andersen, W. S. Bickel, R. Boleu, K. Jensen, and E. Veje, *Phys. Scr.* **3**, 255 (1971).

<sup>8</sup>A. Lindgård and S. E. Nielsen, *At. Data Nucl. Data Tables* **19**, 533 (1977).

<sup>9</sup>Y. Baudinet-Robinet, P. D. Dumont, and H. P. Garnier (unpublished).

<sup>10</sup>E. Veje, *Phys. Rev. A* **14**, 2077 (1976).

<sup>11</sup>M. Barat and W. Lichten, *Phys. Rev. A* **6**, 211 (1972).

<sup>12</sup>J. S. Briggs, *Rep. Prog. Phys.* **39**, 217 (1976).

<sup>13</sup>E. Wigner, *Nachr. Ges. Wiss. Göttingen, Math. Phys. Kl.*, 375 (1927).

<sup>14</sup>Y. Baudinet-Robinet (private communication).

<sup>15</sup>J. Lenormand, *J. Phys. (Paris)* **37**, 699 (1976); L. Wolterbeek Muller and F. J. de Heer, *Physica (Utrecht)* **48**, 345 (1970).

<sup>16</sup>W. G. Baber and H. R. Hassé, *Proc. Cambridge Philos. Soc.* **31**, 564 (1935); L. I. Ponomarev and T. P. Puzynina, *Zh. Eksp. Teor. Fiz.* **52**, 1273 (1967) [*Sov. Phys.—JETP* **25**, 846 (1967)]; K. Helfrich and H. Hartmann, *Theor. Chim. Acta* **16**, 263 (1970).

<sup>17</sup>H. Rosenthal and H. M. Foley, *Phys. Rev. Lett.* **23**, 1480 (1969); H. Rosenthal, *Phys. Rev. A* **4**, 1030 (1971).

<sup>18</sup>V. A. Ankudinov, S. V. Bobashev, and V. I. Perel, *Zh. Eksp. Teor. Fiz.* **60**, 906 (1971) [*Sov. Phys.—JETP* **33**, 490 (1971)]. S. V. Bobashev, in *Physics of Electronic and Atomic Collisions, Invited Lectures and Progress Reports of the Seventh International Conference on the Physics of Electronic and Atomic Collisions, Amsterdam 1971*, edited by L. M. Branscomb *et al.* (North-Holland, Amsterdam, 1972), p. 38.

<sup>19</sup>B. Andresen, K. Jensen, and E. Veje, *Phys. Rev. A* **16**, 150 (1977).

<sup>20</sup>N. H. Tolk, J. C. Tully, J. Kraus, C. W. White, and S. H. Neff, *Phys. Rev. Lett.* **36**, 747 (1976).

<sup>21</sup>H. H. Brongersmar and T. M. Buck, *Nucl. Instrum. Methods* **132**, 599 (1976).

<sup>22</sup>A. Zartner, E. Taglauer, and W. Heiland, *Phys. Rev. Lett.* **40**, 1259 (1978).